THE JOURNAL OF PHYSICAL CHEMISTRY B

Article

pubs.acs.org/JPCB

Formation Mechanism and Possible Stereocontrol of Bisphenol A Derivatives: A Computational Study

Swastika Banerjee,[†,‡] Ganga Periyasamy,[∥] and Swapan K. Pati*[,†,‡,§]

[†]New Chemistry Unit, Bangalore 560064, India

[‡]Jawaharlal Nehru Center for Advanced Scientific Research, Bangalore 560064, India

[§]Theoretical Sciences Unit and [∥]Chemistry Department, Bangalore University, Bangalore 560056, India

Supporting Information

ABSTRACT: Density functional theoretical study elucidates two different pathways for metabolic activation of 2,2′-bis(4-hydroxyphenyl) propane (Bisphenol A; BPA) and consequential formation of 4-methyl-2,4-bis(*p*-hydroxyphenyl)pent-2-ene (M-1) and 4-methyl-2,4-bis(4-hydroxyphenyl)pent-1-ene (M-2, the potential environmental estrogen). Selectivity toward M-1(nontoxic)/M-2(toxic) formation can be controlled by varying the polarity of the reaction medium. We also found the reversal of thermodynamic stability for M-1/M-2 in response to the static polarization of the medium. Moreover, stereocontrol of biologically active M-2 with static polarization as the switch (∼0.005 au) might affect the receptor binding. This analysis may be useful in dictating the prevention of the harmful action of BPA and its metabolites.

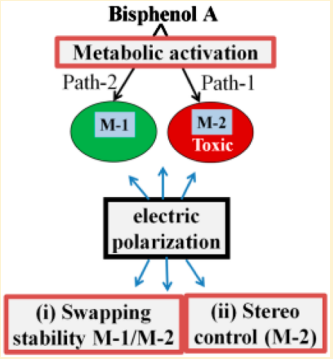

BPA, a component of polycarbonate plastics and epoxy resins,[1−4] which are used in commercial products like coatings and liners of food containers,[5,6] is a part of our daily life. In fact, Tetrabromobisphenol A (TBBPA) is the most widely used brominated flame retardant (BFR). It is an excellent molecule that reduces the flammability of plastics and textile applications, for example, electronics, clothes, and furniture. This compound also degrades to Bisphenol A (BPA) and to an ether derivative of TBBPA (TBBPA-dimethyl-ether). These (TBBPA and its derivatives convert to BPA in the cycle of events) act as a potential source of pollutants in the environment.[7−9] In fact, the toxicity of BPA is often linked with the fact that its cage structure is very similar to that of dioxins (PCDD/Fs) compounds. This feature enlightens the fact that stereocontrol is important to control the toxicity. According to earlier studies,[5,10−13] BPA acts as a transcriptional activator of human estrogen receptor (ERα, ERβ) and involves major health risks. It accumulates in nature without decomposition, causing neurotoxicity and reproductive damage in living organisms.[14−16] Low levels of BPA are detected in 90% of human urine samples, indicating that exposure to BPA is widespread. Surprisingly, a predominant metabolite of BPA, called BPA monoglucuronide, is an inactive estrogen.[17] Hence, BPA's potential health issues demand our understanding of the underlying mechanism behind its toxicity. When glucuronidation is unable to work as a detoxification pathway of BPA, metabolic activation occurs,[18] thereby producing two constitutional (structural) isomers with molecular formula ($C_{18}H_{20}O_2$), M-1 and M-2, as shown in Scheme 1. Importantly, recent endeavors[19,20] emphasize the fact that neither BPA nor M-1 but M-2 is the potential

Scheme 1. Possible Mechanistic Pathway for the Formation of M-1 and M-2 from BPA

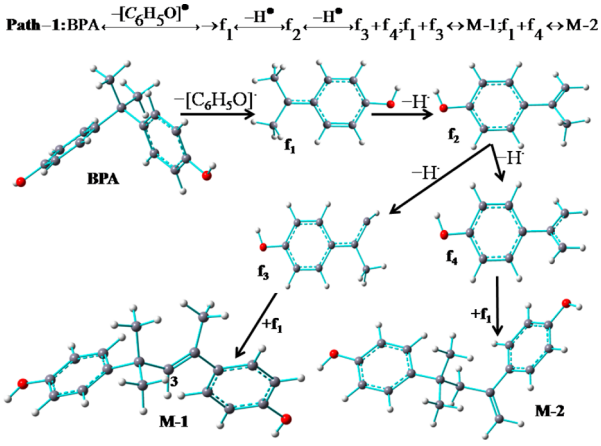

environmental estrogen because of its activity at nM concentration. The appropriate spacing of two terminal phenolic moieties and a middle aliphatic spacer group triggers M-2 to act as a potential disruptor toward the estrogen receptors (ERα and ERβ).[21] However, the possibilities of controlling the selective formation and the detrimental action of toxic metabolite (M-2) are not well-known. Hence, computational studies have been employed to understand the electronic structural factors influencing the mechanistic path-

Received: July 9, 2014
Published: July 11, 2014

   dx.doi.org/10.1021/jp506822w | J. Phys. Chem. B 2014, 118, 9258−9262

way and the conformational features of biologically active M-2. In this context, previous studies on external-perturbation-induced conformational regulation of biological systems,[22] modulation of neuronal ion channels,[19,23,24] and protein targeting[25] are insightful. Here, we present a thorough investigation of the switching of the relative stability of BPA metabolites (isomeric M-1 and M-2) and the control over the conformation of the toxic metabolite (M-2) by external perturbation.

We suggest the mechanistic pathway for BPA metabolic activation, based on experimental findings as described in previous study[15] and our electronic structure calculations. The geometries of the reactants, intermediates, transition states, and products according to Schemes 1 and 2 are optimized using

Scheme 2. M-1 formation Involving Another Set of Precursor Radicals

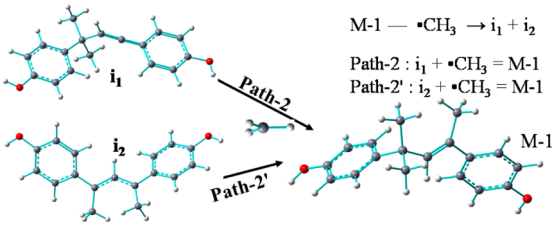

B3LYP as well as M06-2X functionals[26−33] with the 6-311+G (d, p) basis set.[34] Three different implicit solvent models of different dielectric constants (low (ε = 1), intermediate (ε = 46), and high (ε = 88)) have also been considered. Gaussian 09 programs are used for the density functional theory (DFT) calculations.[35−37] ^{1}H NMR peaks for M-2 have been calculated. There is excellent agreement between experimental and computational ^{1}H NMR peaks (see Table T1 in the Supporting Information (SI)). Further details of methodology have been discussed in the SI. Our calculations also corroborate with previous experimental findings,[18] which agree with the fact that the recombination of radical precursors to form M-1 and M-2 complexes is thermodynamically more favorable than the recombination of ionic fragments. In this article, instead of dealing with recombination processes, which have already been experimentally determined, we focus on the kinetically favored path and the possibility of the thermodynamic stereocontrol. Two possible schemes (Schemes 1 and 2) are developed to understand the metabolic activation of BPA. These two schemes are well supported by the LC/MS/MS analysis of BPA metabolites (M-1 and M-2).[18] Our initial calculations have been carried out with the hybrid functional (B3LYP) and triple-ζ basis set including polarization as well as the diffusive nature of the atomic orbitals. This method is well verified, and the size of the basis set is good enough to study the energetics of such small purely organic molecules. In fact, using this functional, we find a negative free energy of formation of M-1 and M-2. As the metabolic activation happens under physiological conditions, we have provided the result that corresponds to the water solvent media.

However, there are some recent theoretical advances and experimental evidence showing the poor performance of B3LYP in predicting reaction barriers.[38] The meta-hybrid-GGA functional M06-2X overcomes this problem associated with B3LYP to an appreciable extent. Hence, we have reconsidered our computational findings with M06-2X for predicting the reaction enthalpy as well as free-energy barriers, including the rate constants and entropic contribution toward the reaction kinetics (see Tables 1 and 2).

Table 1. Computed Activation Barrier for Various Pathways in Terms of the Enthalpy ($\Delta H^{\#}$) and Free Energy ($\Delta G^{\#}$, in kcal mol^{-1})[a]

		$\Delta H^{\#}$; $\Delta G^{\#}$ (kcal/mol)		
path	complex formed	ε = 1	ε = 46	ε = 88
path-1	M-1	37.6 (4.8); 50.2 (17.8)	11.5 (16.1); 27.6(18.3)	11.5 (16.1); 27.5 (17.3)
	M-2	27.4(16.7); 40.2(28.5)	28.1 (17.9); 41.5(30.1)	28.1 (17.9); 41.5(30.1)
path-2	M-1	21.6 (9.7); 33.0(20.7)	13.3(4.5); 20.2(14. 9)	15.9(10.1); 10.3(20.6)
path-2′	M-1	65.5; 81.8	67.6; 82.5	67.8; 80.5

[a]Values shown in the table have been computed at B3LYP/6-311+G(d,p), and the values within the parentheses are the quantities obtained with M06-2X/6-311+G(d,p).

Table 2. Entropy Change Associated with the Formation of Transition States in Different Paths ($\Delta S^{\#}$ in cal mol^{-1}) and the Reaction Rate Constant (k) at T = 298 K in s^{-1} (k(298))

		$\Delta S^{\#}$ (cal/mol); k(298) (s^{-1})		
path	complex formed	ε = 1	ε = 46	ε = 88
path-1	M-1	−45.0; 0.557	−7.9; 0.216	−4.3; 1.211
	M-2	−41.1; 7.456×10^{-7}	−42.3; 0.527×10^{-9}	−42.3; 0.518×10^{-9}
path-2	M-1	−38.1; 0.004	−36.0; 7.318	−36.1; 0.005

The overall reaction appears to be the following: 2 mol of BPA produced 2 mol of phenol and 1 mol of M-1/M-2. A negative free energy shows that formation of M-1 and M-2 is thermodynamically favorable; ΔG: −31.1 (M-1); −27.2 (M-2) kcal mol^{-1} (in a water dielectric medium).

According to Scheme 1, BPA degrades into two radical fragments, f_1 and phenolic radical. Rearrangement of f_1 is followed by the elimination of acidic H$^{\bullet}$, thereby forming f_3 and f_4 radicals, which remain in the medium along with the residuals f_1 and f_2. These fragment radicals (shown in Scheme 1.) are chemically stable with a larger HOMO−LUMO gap (see Table T2 in the SI), resulting in a finite lifetime. This facilitates the occurrence of sequential steps (Scheme 1). Extensive calculations prove that the combinations of f_3 and f_4 radicals with f_2 are the rate-determining steps for formation of M-1 and M-2, respectively.

However, spectroscopic evidence[18] for the sustainability of i_1 and i_2 (molecular weight = 252) radicals from mass spectrometric analysis points toward the presence of another set of radical fragments as reactants for path-2 and path-2′ (see Scheme 2). Here, i_1 and i_2 are interconvertible through intramolecular methyl group transfer. Thus, three different sets of precursor radicals (see path-1, path-2, and path-2′) participate in M-1 formation, whereas for M-2, only one set of radical precursors is involved (see path-1). Hence, the activation (enthalpy and free energy) barrier for the formation of M-1 and M-2 is essential to predict the most favorable pathway among the possibilities. Because this metabolic process happens in physiological conditions, we have included different

dx.doi.org/10.1021/jp506822w | J. Phys. Chem. B 2014, 118, 9258−9262

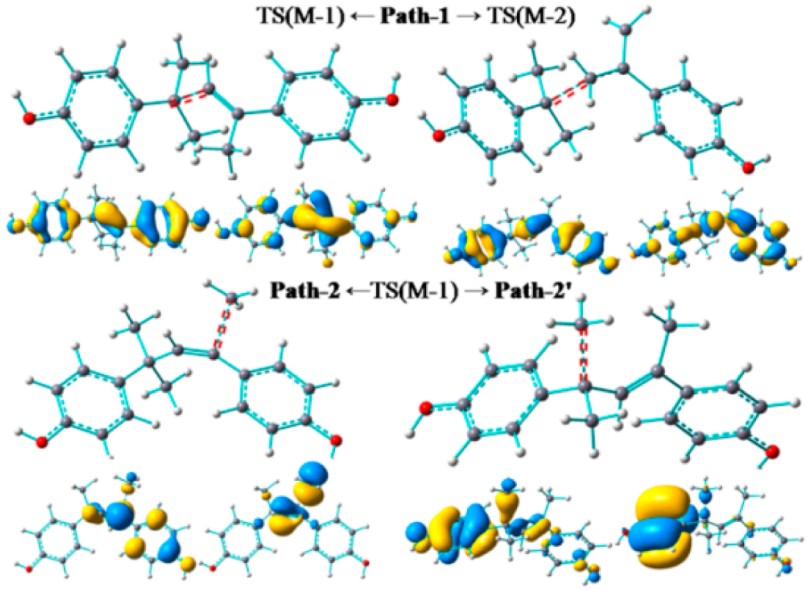

Figure 1. B3LYP/6-311+G (d,P)/PCM optimized transition-state geometries of the rate-determining steps for M-1 and M-2 formation. Transition orbital are also shown.

dielectric media to mimic the solvent environment to assess the thermodynamic stability and kinetic feasibility.

The significant difference in reaction activation free energy and enthalpy barriers shown in Table 1 reveals the striking role of entropy changes during reaction. In fact, the entropy decreases substantially due to the formation of a transition state after the combination of radical precursors (see Table 2). The entropic effect is comparatively less important in the case of M-1 formation via path-1 in a medium with a high dielectric constant. Moreover, the formation of M-1 and M-2 involves a polar transition state (see Figure 1), which is reflected in the pronounced sensitivity of the transition-state energy barrier (see Table 1) and rate constant (see Table 2) to the different polar environments. Although the fundamental conclusions on favored paths and control over the reaction rates based on B3LYP calculations are very corroborative with the findings using the M06-2X functional, there is a difference in quantitative values for the activation energy barrier. While both set of results agree well with each other, predicting the possibility for path-2 toward the formation of M-1, the computed activation energy barriers using M06-2X appear to be lower in comparison with B3LYP. This is due to the increase in the relative stability of the transition state with the consideration of a highly nonlocal functional with a double amount of nonlocal exchange (in M06-2X). The difference in the reaction energy barrier is expected because proper consideration of the treatment of the orbital transition ($\pi-\sigma$) and asynchronicity associated with the activation have been treated differently for two different density functionals.[38] Interestingly, we conclude that the transition-state geometry does not differ for both functionals, showing its robustness. We also infer that both path-1 and path-2 ($k(298)$ in s^{-1}: 7.318 at ε = 46 for path-1; 1.211 at ε =88 for path-2) are favored for M-1 formation (see Table 2), whereas M-2 formation appears to be preferred via path-1 with a rate constant of $k(298) = 7.456 \times 10^{-7}$ s^{-1} in a medium with low dielectric constant. Fascinatingly, the increase in the dielectric constant (ε) of the medium boosts the selective formation of less toxic M-1 (see Tables 1 and 2).

Relative stability of BPA metabolites (M-1 and M-2) has been studied at different solvent polarities (see Table T3 in the SI). However, the relative stability change is in the energy range of thermal processes at room temperature. This reveals equal stability of M-1/M-2 in various implicit solvent considerations. Therefore, polarizable continuum solvation is unable to selectively stabilize one over another. Hence, the responses of M-1 and M-2 are studied in the presence of static electrical polarization to investigate the possibility of electrical polarization as a switch to control their relative stability. To study the response (of M-1 and M-2) to external uniform static electric fields, we perform density functional theory computations with a highly diffused and polarizable basis set (see the SI). We have considered fields in the range of 0−0.01 au (to avoid numerically very large field strengths; 0.01 au of the electric field = 0.5142 V/Å).

Figure 2 reveals that the stability of M-1 and M-2 can be swapped by controlling the static electric polarization in media.

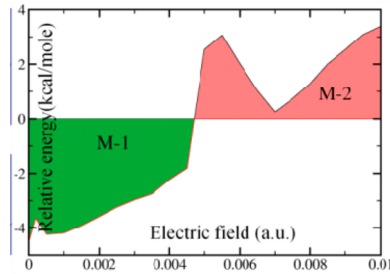

Relative energy (Electronic)

Figure 2. Relative energy (electronic energy (M-1) − electronic energy (M-2)) shown under the influence of uniform various static electric polarization.

M-1 becomes preferential below a threshold value of ∼0.005 au. We believe that this is an appropriate direction for alteration of the relative stability of M-1 and M-2. In order to understand this different response of M-1 and M-2 to an external electric field, we focus on their inherent polarization (see the electrostatic potential map in SI Figure S3), which is

dx.doi.org/10.1021/jp506822w | J. Phys. Chem. B 2014, 118, 9258−9262

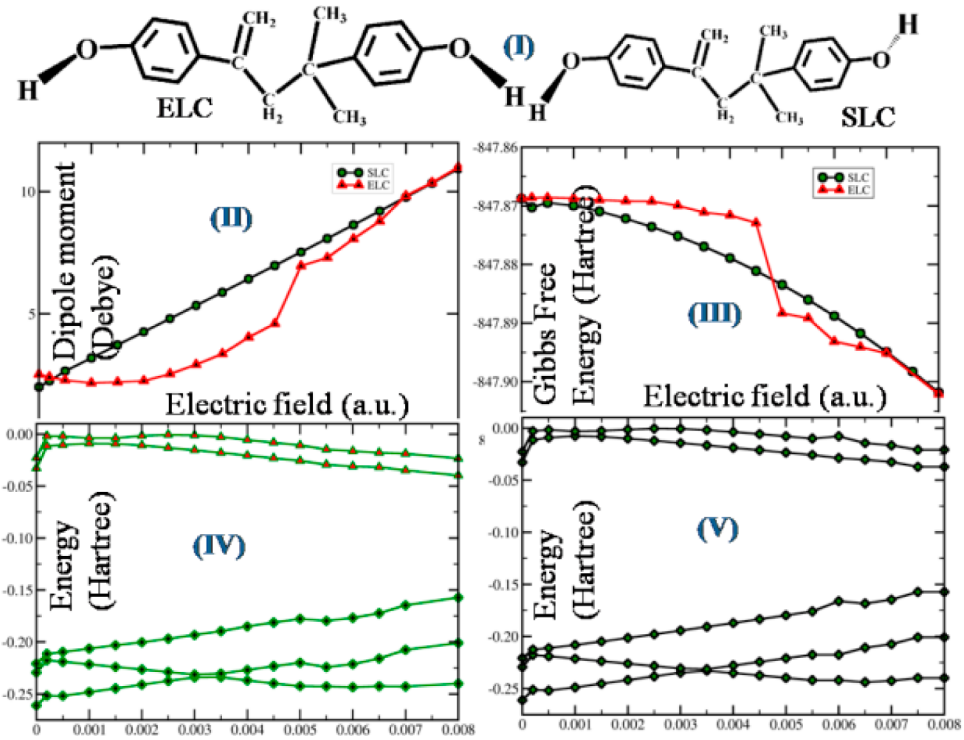

Figure 3. (I) Two conformers of M-2 (ELC and SLC); (II) their different responses in the electric dipole moment; (III) free energy responses; (IV) energetics of electronic states (from bottom to top starting from HOMO−2 up to LUMO+1) of the ELC; and (V) for SLC under the influence of uniform static electric polarization.

significantly different for M-1 and M-2. In fact, M-1 and M-2 possess different π delocalization patterns; hence, the electric field polarizes them differently and brings out the discrepancy in electronic redistribution and stabilization. Therefore, static electric polarization controlling the relative stability of M-1 over M-2 and vice versa can be used as a "switch", which occurs at a very small field strength (~0.005 au ≈ 0.26 V/Å).

An optimum conformational feature (terminal O−H bond orientation, molecular length) of M-2 is a crucial factor for its receptor binding. Hence, we focus on the possible stereocontrol of a toxic metabolite (M-2). Detailed conformational analyses reveal that M-2 exhibits two possible orientations of the terminal O−H (short length conformer: SLC and extended length conformer: ELC, shown in Figure 3I). They are energetically equal but strikingly have different molecular lengths (difference: ~1 Å) and dipole moments (difference: ~0.51 D). The interaction of an overall electrically neutral polar species (net dipole moment = μ) with an imposed electric field of strength (F) comes through a dipole interaction given by $-\mu \cdot F$. This interaction favors alignment of individual bond dipoles along the field direction and promotes electronic redistribution. Figure 3II shows that the dipole moment increases smoothly with an increase in external perturbation with a constant slope for SLC but not for ELC. An abrupt increase in the dipole moment of ELC (~0.005 au) is followed by equalization in dipole moments and the free energy with SLC, after 0.007 au (see Figure 3II and III). At a critical electric field value (0.003 au), their HOMO−LUMO gap remains large, but the gap between HOMO−1 and HOMO−2 tends to zero (see Figure 3IV). Moreover, NBO analysis discloses that individual bond orders are not affected (at <0.01 au), ensuring that the lower electric field strength does not cause fragmentation/structural breakdown but confers conformational switching with (a) changes in the effective length of the molecule and (b) dihedral angle changes in the linker aliphatic group. Thus, selective stabilization of one (between ELC and SLC) is found to be possible through regulation of static electric polarization. This might be considered as a powerful tool to control the simultaneous binding of two terminal phenolic groups to the receptor utilizing an effective alteration of the overall length of M-2. On the other hand, closing of the frontier molecular energy levels (HOMO and LUMO), leading to destabilization and fragmentation, occurs at a high enough field strength (see Figure S4 in the SI). Hence, redistribution of electron density culminates into a catastrophic structural breakdown beyond a specific threshold field strength (0.018 au). Electronic structural changes are found to be accompanied by an abrupt increase in the electric dipole moment, showing a transition point (0.018 au). Thus, uniform static electric polarization becomes a powerful tool for conformational switching and structural evolution of M-2, depending on the choice of strength of external polarizations.

In summary, DFT calculations along with corroborative experimental findings[18] elucidate that the solvent polarity and nature of radical intermediates determines different reaction pathways of metabolic activation. Harmful metabolite (M-2) formation decreases with an increase in the dielectric constant (ε) of the environment (solvent). Sensitivity toward static polarization offers experimental possibilities to achieve reversible switching between a biologically active (M-2) and an inactive state (M-1). Hence, the critical value of the field strength is found to be ~0.005 au. Our work also points toward the conformational change of M-2, which in turn can affect binding to the receptor.

dx.doi.org/10.1021/jp506822w | J. Phys. Chem. B 2014, 118, 9258−9262

■ ASSOCIATED CONTENT

Supporting Information

Detailed computational methodology and computationally found ^{1}H NMR (ppm), effect of the dielectric constant (ε) of the solvent environment on the HOMO−LUMO energy gap (H−L), effect of the dielectric constant (ε) of the solvent environment on the relative stability for various precursor radicals, molecular electrostatic potential mapped on the total electron density, different responses in the electric dipole moment to the uniform electric field. This material is available free of charge via the Internet at http://pubs.acs.org.

■ AUTHOR INFORMATION

Corresponding Author

*E-mail: swapan.jnc@gmail.com.

Notes

The authors declare no competing financial interest.

■ ACKNOWLEDGMENTS

S.B. acknowledges CSIR, Govt. of India for a senior research fellowship, and G.P. thanks the DST-Women scientist fellowship. S.K.P. acknowledges the DST (Government of India) and AOARD, U.S. Air Force, for a research grant.

■ REFERENCES

(1) Wang, H. L.; Toppare, L.; Fernandez, J. E. *Macromolecules* **1990**, *23*, 1053−1059.
(2) Dondoni, A.; Ghiglione, C.; Marra, A.; Scoponi, M. *Chem. Commun.* **1997**, 673−674.
(3) Das, D.; Lee, J.-F.; Cheng, S. *Chem. Commun.* **2001**, 2178−2179.
(4) Liu, Z.; Zhang, X.; Poyraz, S.; Surwade, S. P.; Manohar, S. K. *J. Am. Chem. Soc.* **2010**, *132*, 13158−13159.
(5) Krishnan, A. V.; Stathis, P.; Permuth, S. F.; Tokes, L.; Feldman, D. *Endocrinology* **1993**, *132*, 2279−2286.
(6) Dowling, K. C.; Thomas, J. K. *Macromolecules* **1990**, *23*, 1059−1064.
(7) Alaee, M.; Arias, P.; Sjödin, A.; Bergman, Ã. k. *Environ. Int.* **2003**, *29*, 683−689.
(8) Geyer, H. J.; Schramm, K.-W.; Darnerud, P. O.; Aune, M.; Feicht, E. A.; Fried, K. W.; Henkelmann, B.; Lenoir, D.; Schmid, P.; McDonald, T. A. *Organohalogen Compd.* **2004**, *66*, 3867−3872.
(9) Hamers, T.; Kamstra, J. H.; Sonneveld, E.; Murk, A. J.; Kester, M. H. A.; Andersson, P. L.; Legler, J.; Brouwer, A. *Toxicol. Sci.* **2006**, *92*, 157−173.
(10) Tabata, A.; Kashiwada, S.; Ohnishi, Y.; Ishikawa, H.; Miyamoto, N.; Itoh, M.; Magara, Y. *Water Sci. Technol.* **2001**, *43*, 109−116.
(11) Eriksson, P.; Jakobsson, E.; Fredriksson, A. *Organohalogen Compd.* **1998**, *35*, 375.
(12) Staples, C. A.; Dome, P. B.; Klecka, G. M.; Oblock, S. T.; Harris, L. R. *Chemosphere* **1998**, *36*, 2149−2173.
(13) Shen, X.; Zhu, L.; Wang, N.; Ye, L.; Tang, H. *Chem. Commun.* **2012**, *48*, 788−798.
(14) Atkinson, A.; Roy, D. *Environ. Mol. Mutagen.* **1995**, *26*, 60−66.
(15) Roy, D.; Palangat, M.; Chen, C.-W.; Thomas, R. D.; Colerangle, J.; Atkinson, A.; Yan, Z.-J. *J. Toxicol. Environ. Health, Part A* **1997**, *50*, 1−30.
(16) Ben-Jonathan, N.; Steinmetz, R. *Trends Endocrinol. Metab.* **1998**, *9*, 124−128.
(17) Matthews, J. B.; Twomey, K.; Zacharewski, T. R. *Chem. Res. Toxicol.* **2001**, *14*, 149−157.
(18) Yoshihara, S. i.; Mizutare, T.; Makishima, M.; Suzuki, N.; Fujimoto, N.; Igarashi, K.; Ohta, S. *Toxicol. Sci.* **2004**, *78*, 50−59.
(19) Mu, X.; Rider, C. V.; Hwang, G. S.; Hoy, H.; LeBlanc, G. A. *Environ. Toxicol. Chem.* **2005**, *24*, 146−152.
(20) Baker, M. E.; Chandsawangbhuwana, C. *PloS One* **2012**, *7*, e46078.
(21) Pettersson, K.; Gustafsson, J.-Ã. k. *Annu. Rev. Physiol.* **2001**, *63*, 165−192.
(22) Hall, J. M.; McDonnell, D. P.; Korach, K. S. *Mol. Endocrinol.* **2002**, *16*, 469−486.
(23) Stierl, M.; Stumpf, P.; Udwari, D.; Gueta, R.; Hagedorn, R.; Losi, A.; Gärtner, W.; Petereit, L.; Efetova, M.; Schwarzel, M. *J. Biol. Chem.* **2011**, *286*, 1181−1188.
(24) Mayer, G. n.; Heckel, A. *Angew. Chem., Int. Ed.* **2006**, *45*, 4900−4921.
(25) Walter, P.; Johnson, A. E. *Annu. Rev. Cell Biol.* **1994**, *10*, 87−119.
(26) Ernzerhof, M.; Scuseria, G. E. *J. Chem. Phys.* **1999**, *110*, 5029−5036.
(27) Yanai, T.; Tew, D. P.; Handy, N. C. *Chem. Phys. Lett.* **2004**, *393*, 51−57.
(28) Bilc, D. I.; Orlando, R.; Shaltaf, R.; Rignanese, G. M.; Íñiguez, J.; Ghosez, P. *Phys. Rev. B* **2008**, *77*, 165107.
(29) Frisch, M.; Trucks, G. W.; Schlegel, H. B.; Scuseria, G. E.; Robb, M. A.; Cheeseman, J. R.; Scalmani, G.; Barone, V.; Mennucci, B.; Petersson, G. A.; et al. *Gaussian*; Gaussian Inc., Wallingford, CT, 2009.
(30) Zhao, Y.; Schultz, N. E.; Truhlar, D. G. *J. Chem. Theory Comput.* **2006**, *2*, 364−382.
(31) Zhao, Y.; Truhlar, D. G. *J. Phys. Chem. A* **2006**, *110*, 13126−13130.
(32) Zhao, Y.; Truhlar, D. G. *J. Chem. Phys.* **2006**, *125*, 194101.
(33) Zhao, Y.; Truhlar, D. G. *Theor. Chem. Acc.* **2008**, *120*, 215−241.
(34) Andersson, M. P.; Uvdal, P. *J. Phys. Chem. A* **2005**, *109*, 2937−2941.
(35) Kohn, W.; Becke, A. D.; Parr, R. G. *J. Phys. Chem.* **1996**, *100*, 12974−12980.
(36) Becke, A. D. *J. Chem. Phys.* **1993**, *98*, 5648−5652.
(37) Baboul, A. G.; Curtiss, L. A.; Redfern, P. C.; Raghavachari, K. *J. Chem. Phys.* **1999**, *110*, 7650−7657.
(38) Linder, M.; Brinck, T. *Phys. Chem. Chem. Phys.* **2013**, *15*, 5108−5114.